Supporting Information

Multi-Nanoparticle Model Simulations of the Porosity Effect on Sintering Processes in Ni/YSZ and Ni/ScSZ by Molecular Dynamics Method

Jingxiang Xu,[a] Shandan Bai,[b] Yuji Higuchi,[a] Nobuki Ozawa,[a] Kazuhisa Sato,[c] Toshiyuki Hashida,[c] and Momoji Kubo*[a]

[a]Institute for Materials Research, Tohoku University, 2-1-1 Katahira, Aoba-ku, Sendai 980-8577, Japan

[b]New Industry Creation Hatchery Center, Tohoku University, 6-6-10 Aoba, Aramaki, Aoba-ku, Sendai 980-8579, Japan

[c]Fracture and Reliability Research Institute, Graduate School of Engineering, Tohoku University, 6-6-11 Aoba, Aramaki, Aoba-ku, Sendai 980-8579, Japan

*Corresponding author
Tel: +81-22-215-2050
Fax: +81-22-215-2051
E-mail: momoji@imr.tohoku.ac.jp

Determination of Interatomic Potential Parameters for Ni, YSZ, ScSZ, and Ni/ScSZ

In this study, we used the interatomic potential parameters that were determined and employed in the previous studies.[1,2] The present parameters of Morse and BMH potentials were successfully used to investigate the Ni and ceramic (YSZ, and ScSZ) systems at around 1073K, respectively, in the previous studies.[3-6] They showed that the present parameters of Morse and BMH potentials well reproduce the interactions of the Ni and ceramic (YSZ, and ScSZ), respectively. The melting points of Ni, YSZ, and ScSZ bulks calculated by the MD using the present potential parameters are 2320 K, 5230 K, and 5140 K, respectively. The experimental values for melting points of Ni and YSZ are 1728 K and 3053 K, respectively. Ni, YSZ, and ScSZ lattices in the experiment include many defects and grain boundaries, etc., however, the simulation models of Ni, YSZ, and ScSZ in our MD calculations are perfect lattice. Thus, it is reasonable that the melting points calculated by the MD using the present potential parameters are higher than their experimental values. Actually, it is difficult to obtain the melting point of perfect lattice by the experiment. Furthermore, in this study, all the sintering simulations were performed at 1073 K that is much lower than their melting temperature. Thus, although our melting points of Ni and YSZ calculated by the MD using the present potential parameters are higher than their experimental values, it is suggested that the interatomic potential parameters for Ni, YSZ, and ScSZ do not have significant influence on our simulation in this study.

To validate the parameters using in this study, we calculated the surface and interfacial energies by molecular dynamics (MD) method. The surface energies of Ni, YSZ, and ScSZ are calculated by $\gamma' = (E_{slab} - E_{bulk} \cdot N)/2S$, where E_{slab} is the total energy of the Ni(111), YSZ(111), and ScSZ(111) slabs, E_{bulk} is the reference energy for a Ni, YSZ, and ScSZ unit in bulk phase, N is the number of Ni, YSZ, and ScSZ units in the Ni(111), YSZ(111), and ScSZ(111) slabs, and S is the surface area of Ni(111), YSZ(111), and ScSZ(111) slabs. The calculated surface energies of Ni(111), YSZ(111), and ScSZ(111) are 2.10, 1.28, 1.44 $J \cdot m^{-2}$, respectively. The previous experimental study[7] reported that the surface energy of Ni is 2.38 $J \cdot m^{-2}$. The surface energy of Ni calculated by the MD using the present potential parameters is similar to its experimental value. In this study, the calculated surface energy of YSZ is 1.28 $J \cdot m^{-2}$; the experimental value is 1.38 $J \cdot m^{-2}$.[8] Hence, the surface energy of YSZ calculated by the MD using the present potential parameters is similar to its experimental value. In this study, the surface energies of YSZ(111) and ScSZ(111) calculated by the MD using the present potential parameters are 1.28 and 1.44 $J \cdot m^{-2}$, respectively. The previous density functional study[9] reported that the surface energies of YSZ(111) and ScSZ(111) are 0.70 and 0.78 $J \cdot m^{-2}$, respectively. In our MD simulations, the surface energy of YSZ(111) is smaller than that of ScSZ(111), which is consistent with the results calculated by the DFT. Therefore, we conclude that the present interatomic potential parameters are sufficient to reproduce the surface energies.

The interfacial energy of Ni/YSZ is calculated by $\gamma = (E_{Binding} + \gamma'_{Ni} + \gamma'_{YSZ})/S$, where $E_{Binding}$ is equal to $E_{Ni/YSZ} - E_{Ni\,Slab} - E_{YSZ\,slab}$, and $E_{Ni/YSZ}$ is the total energy of the Ni(111)/YSZ(111) (Figure S1a). $E_{Ni\,Slab}$ and $E_{YSZ\,slab}$ are the total energies of YSZ(111) (Figure S1b) and Ni(111) (Figure S1c) slabs. The interfacial energy of Ni/ScSZ is also calculated by the same method. The interfacial energies of Ni/YSZ and Ni/ScSZ calculated by the MD using the present potential parameters are 1.92 and 1.59 $J \cdot m^{-2}$, respectively. Actually, it is difficult to obtain the interfacial energies of the metal/metal oxide interface by the experiment. Then, we calculated the interfacial energies of Ni(111)/YSZ(111) and Ni(111)/ScSZ(111) by the DFT with GGA-PBE functional. The interfacial energies of Ni(111)/YSZ(111) and Ni(111)/ScSZ(111) obtained by DFT calculations are 1.47 and 1.39 J/m^2, respectively; the interfacial energies of Ni(111)/YSZ(111) and Ni(111)/ScSZ(111) calculated by the MD using the present potential parameters are 1.92 and 1.59 J/m^2, respectively. In both results, the interfacial energy of Ni(111)/ScSZ(111) is smaller than that of Ni(111)/YSZ(111). Hence, the interfacial energies by the MD using the present potential parameters are consistent with the results calculated by the DFT. Therefore, we conclude that the present interatomic potential parameters are sufficient to reproduce the interfacial energies.

We used our previous method[10] for determining accurate Morse potential parameters to describe the interaction between Ni and the ScSZ. The interaction energies between Ni and ScSZ were calculated by using the DMol^3 DFT package.[11,12] In the DFT calculations, a generalized gradient approximation using the Perdew–Burke–Ernzerhof[13] correlation functional was applied to the exchange-correlation term in all the calculations. The effective core potentials were used to model the core electrons. The double numerical plus polarization basis sets were used to describe the atomic orbitals. We used one Ni atom on the ScSZ(111) surface as the DFT calculation model (Figure S2). The Ni atom was located on the on-top sites of the Zr, O, and Sc atoms in the ScSZ(111) surface with vertical distance, *R*, to the surface of 1.5 to 5.0 Å at intervals of 0.1 Å. Here, the interaction energy is defined as

$$E = E_{\mathrm{Ni/ScSZ(111)}} - \left(E_{\mathrm{Ni\,atom}} + E_{\mathrm{ScSZ(111)slab}}\right), \quad (1)$$

where E is the interaction energy of the Ni atom and the ScSZ(111) surface; $E_{\mathrm{Ni/ScSZ(111)}}$ is the total energy of the adsorbed Ni atom and the ScSZ(111) surface; and E_{Niatom} and $E_{\mathrm{ScSZ(111)}}$ are the total energies of the isolated Ni atom and the ScSZ(111) surface, respectively.

We divided the interaction energies between Ni and ScSZ obtained from the DFT calculations into three sets of interaction energies (Ni-Zr, Ni-O, and Ni-Sc) to describe the interactions of the Ni/ScSZ system. To fit the potential parameters, the basic Morse potential function is rewritten as the following.

$$
\begin{aligned}
E = & \sum_{\mathrm{Zr}} D_{\mathrm{Ni-Zr}} \{\exp[-2\beta_{\mathrm{Ni-Zr}}(r_{\mathrm{Ni-Zr}} - r^*_{\mathrm{Ni-Zr}})] \\
& - 2\exp[-\beta_{\mathrm{Ni-Zr}}(r_{\mathrm{Ni-Zr}} - r^*_{\mathrm{Ni-Zr}})]\} \\
& + \sum_{\mathrm{O}} D_{\mathrm{Ni-O}} \{\exp[-2\beta_{\mathrm{Ni-O}}(r_{\mathrm{Ni-O}} - r^*_{\mathrm{Ni-O}})] \\
& - 2\exp[-\beta_{\mathrm{Ni-O}}(r_{\mathrm{Ni-O}} - r^*_{\mathrm{Ni-O}})]\} \\
& + \sum_{\mathrm{Sc}} D_{\mathrm{Ni-Sc}} \{\exp[-2\beta_{\mathrm{Ni-Sc}}(r_{\mathrm{Ni-Sc}} - r^*_{\mathrm{Ni-Sc}})] \\
& - 2\exp[-\beta_{\mathrm{Ni-Sc}}(r_{\mathrm{Ni-Sc}} - r^*_{\mathrm{Ni-Sc}})]\}
\end{aligned} \tag{2}
$$

Here, the parameters D_{Ni-X}, β_{Ni-X}, and r^*_{Ni-X} are related to the bond energy, stiffness, and the bond length between Ni and X, respectively. In this, X represents any atom in the ScSZ(111) surface (Zr, O, or Sc). The three sets of interaction energies, *E*, were obtained as a function of the vertical distance between the Ni atom and the ScSZ(111) surface. The least-squares criterion for fitting is defined as

$$
\min\left\{\sum_{site}\sum_{R}(E_{fit} - E_{DFT})^2\right\}, \tag{3}
$$

where *R* is the vertical distance between the Ni atom and the sites on the ScSZ(111) surface, and E_{fit} and E_{DFT} are the interaction energy values obtained by fitting the Morse potential and from the DFT calculations, respectively. The two sets (Ni-O and Ni-Zr) of potential parameters were already determined in our previous study.[10] Here, we need to determine the set of potential parameters only between Ni and Sc, because the potential parameters for Ni-O and Ni-Zr in the Ni/ScSZ system should be consistent with those in the Ni/YSZ system. The Levenberg–Marquardt method[14,15] was used to solve the test function (Eq. 3) and determine the parameters *D*, *β*, and r^*, which are related to the bond energy, stiffness, and bond length, respectively, of the Ni-Sc bond in the rewritten Morse functions (Eq. 2). The periodic boundary condition within the cutoff value corresponding to half of the unit cell length was employed. The fitting is based on Eq. 3 with the interaction energies at 12, 12, and 11 points for the on-top sites of the O, Zr, and Sc atoms in the ScSZ(111) surface. The determined DFT-based potential parameters for Ni and ScSZ are listed in Table 3. The dependence of the interaction energies on the distance between the Ni atom and the ScSZ(111) surface at three sites is shown in Figure S3. The fitted Morse potential curves accurately reproduced the DFT interaction energies at 35 points for the on-top sites of the O, Zr, and Sc atoms in the ScSZ(111) surface. The r^*_{ij} values related to the Ni-Zr, Ni-Y, and Ni-Sc bond lengths are 3.80, 4.17, and 3.96 Å, respectively; the experimental ionic radii of Zr^{4+}, Y^{3+}, and Sc^{3+} are 0.84, 1.02, and 0.87 Å, respectively.[16] Hence, the order of the

parameters related to the ionic bond length is consistent with the experimental values of the ionic radii of Zr^{4+}, Y^{3+}, and Sc^{3+}.

Modeling of YSZ and ScSZ Nanoparticles

In our multi-nanoparticle modeling method, the ceramic (YSZ and ScSZ) nanoparticles were obtained by cutting the ceramic (YSZ and ScSZ) bulk as a sphere. We used the ceramic (YSZ and ScSZ) supercell by 10×10×10 as the bulk. The atoms whose distance from the center of the bulk is smaller than or equal to 20 Å construct the sphere. Figure S5 shows the surface structures of YSZ nanoparticle with a diameter of 40 Å obtained by our method. The (111), (110), and (100) planes are observed in Figure S5. The surface structures of YSZ nanoparticle mainly consists of the (111), (110), and (100) planes, which are reported by both experiments[17-19] and density functional theory calculation.[20] Thus, our method is effective to model the (111), (110), and (100) planes of ceramic nanoparticles and our model can reflect the effect of the surface structures of ceramic nanoparticles on the sintering.

Supporting Figures

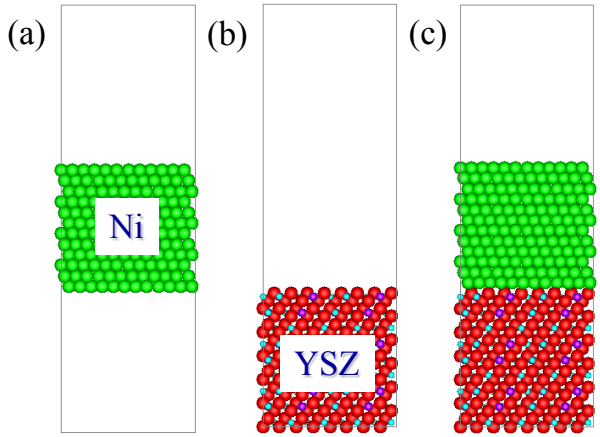

Figure S1. Models for calculating surface energies of (a) Ni(111) slab and (b) YSZ(111) slab, and interfacial energy of (c) Ni(111)/YSZ(111).

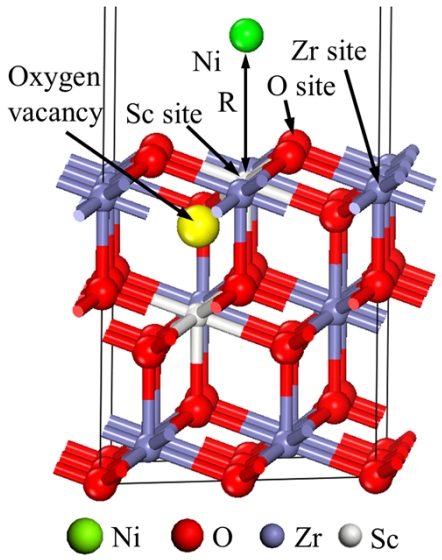

Figure S2. Front view of one Ni atom on the ScSZ(111) surface. The interaction energies were calculated for each distance, R, at each site. R is the vertical distance between the Ni atom and sites on the ScSZ(111) surface from 1.5 to 5.0 Å.

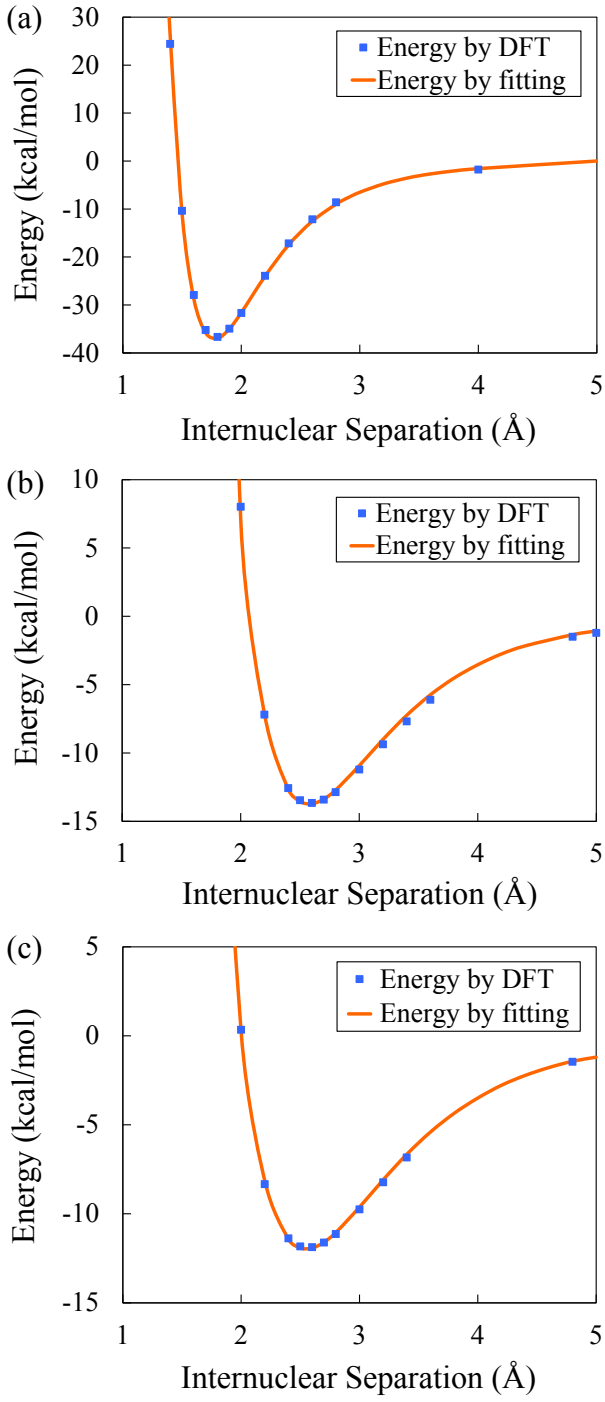

Figure S3. Interaction energies obtained from the DFT calculations and the fitted Morse potential curve of the Ni atom at (a) O, (b) Zr, and (c) Sc sites. The squares and the solid line indicate the interaction energies obtained by the DFT calculations and the potential curves determined by the least-squares fitting method.

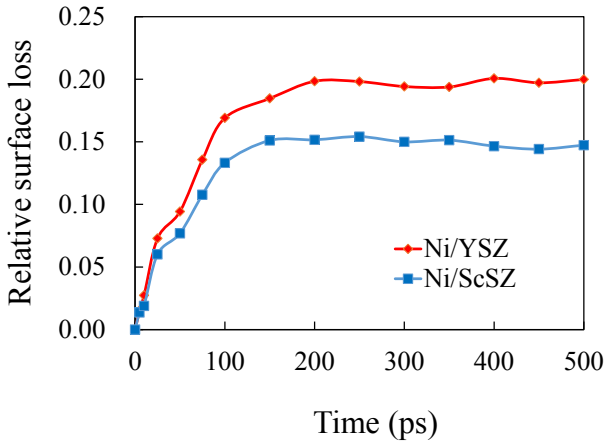

Figure S4. Time evolution of the relative surface loss at 1073 K in the Ni/YSZ and Ni/ScSZ multi-nanoparticle models whose size of Ni and ceramic (YSZ and ScSZ) nanoparticles is 48 Å.

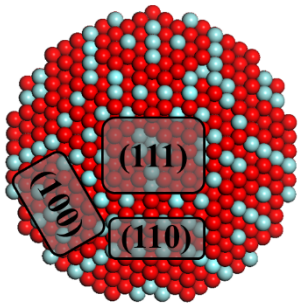

Figure S5. Surface structures of YSZ nanoparticle with a diameter of 40 Å.

References

(1) K. Suzuki et al., *Appl. Phys. Lett.* 1998, **73**, 1502– 1504.
(2) L. A. Girifalco et al., *Phys. Rev.*, 1959, **114**, 687-690.
(3) G. M. Poletaev et al., *Phys. Solid State*, 2009, **51**, 727-732.
(4) N. N. Nedialkov et al., *Appl. Surf. Sci*., 2005, **247**, 243-248.
(5) W. Araki et al., *Solid State Ionics*, 2010, **181**, 1534–1541.
(6) K. L. Tung et al., *Sep. Purif. Technol.*, 2010, **73**, 13-19.
(7) W. R. Tyson et al., *Surf. Sci*., 1977, **62**, 267-276.
(8) A. Tsoga et al., *J. Mater. Sci*., 1996, **31**, 5409–5413.
(9) Z. Zeng et al., *Phys. Chem. Chem. Phys.*, 2013, **15**, 6769-6772.
(10) J. Xu et al., *J. Phys. Chem. C*, 2013, **117**, 9663–9672.
(11) B. Delley, *J. Chem. Phys*., 1990, **92**, 508–517.
(12) B. Delley, *J. Chem. Phys*., 2000, **113**, 7756–7764.

(13) J. P. Perdew et al., *Phys. Rev. Lett*., 1996, **77**, 3865–3868.
(14) K. Levenberg, *Quart. Appl. Math.*, 1944, **2**, 164–168.
(15) D. W. Marquardt, *J. Soc. Ind. Appl. Math*., 1963, **11**, 431–441.
(16) D. R. Lide, CRC Handbook of Chemistry and Physics, 90th ed.; CRC press: Boca Raton, FL, 2009.
(17) T. Thome et al., *J. Eur. Ceram. Soc*., 2004, **24**, 841-846.
(18) X. G. Wang, *Surf. Sci*., 2008, **602**, L5-L9.
(19) S. S. Liu et al., *J. Electrochem. Soc*., 2015, **162**, F750-F754.
(20) G. Ballabio et al., *Phys. Rev. B*, 2004, **70**, 075417.